(Abstract submitted to the 34th IWWWFB, Newcastle, Australia, 2019)

Wave interaction with a shallowly submerged step.

Guy McCauley[a*], Hugh Wolgamot[a], Scott Draper[a] and Jana Orszaghova[a].
[a]Oceans Graduate School, the University of Western Australia, Perth, WA, Australia.
[*]Email: *guy.mccauley@research.uwa.edu.au*

1 Introduction

Some offshore structures, breakwaters or wave energy devices sit shallowly submerged beneath the free surface. When waves interact with such a shallow structure they can break, form bores and generate significant higher harmonic free waves in the lee of the structure. This work is motivated by the Carnegie Clean Energy CETO wave energy device, an ≈25m diameter thin vertical axis cylinder which sits 2-3m submerged below the mean free surface. For surface-piercing devices, parametric studies with linear hydrodynamic models are a key tool; for shallowly submerged devices linear theory may be inadequate due to the effects described above. It is of interest to create computationally efficient models using simplified non-linear equations, that may predict the bulk flow properties adequately for parametric design studies. This work aims to assess the suitability of one such simplified numerical model for waves passing over a shallowly submerged step in 2D. The hybrid model uses linear potential flow in the deep water region and the Non-linear Shallow Water Equations (NSWE) for wave propagation in the shallow water region.

Grue (1992) conducted wave flume experiments examining the higher harmonics generated by regular waves passing over a submerged 2D step. Grue also compared the experiments to a hybrid numerical model using the Boussinesq equations above the step, matched to linear potential flow either side by using a source term at the interfaces. This work considered relatively small amplitude incident waves, from $A_{in}/s = 0.015 - 0.24$, where A_{in} is the incident wave amplitude and s is the step submergence. The wave steepness range in the deeper water region was $kA_{in} = 0.00204 - 0.0327$, where k is the deep water wavenumber. The Boussinesq hybrid model worked remarkably well for small wave amplitudes. However it could not simulate scenarios when wave breaking occurred. Recent work by Skene et al. (2018) examined waves breaking onto a zero mean freeboard step of semi-infinite horizontal extent for $kA_{in} = 0.0314 - 0.125$. This work compared a CFD model to a hybrid numerical model using linear potential flow and the NSWE. It was shown that the NSWE could predict bore height and velocities on top of the step away from the edge. For the problem of a shallowly submerged wave energy device, the wave amplitude may easily exceed half the submergence and ks is smaller than in Grue's work. For scenarios such as this, where wave breaking and bore formation play a significant role in the shallow water flow, it is expected that the NSWE will be more accurate than the Boussinesq equations. Additionally, for the CETO geometry, kW (W is the step width) is smaller than for the geometry of Grue's step, so we expect negligible effects of dispersion.

In the present work, the step geometry of Grue is replicated in CFD with the aim of validating the CFD results against Grue's experiments and then extending the CFD model to larger amplitudes for comparison against the NSWE hybrid model. First we will compare the hybrid model to the linear potential flow solution.

2 Hybrid model comparison to linear potential flow

A hybrid model has been implemented using the NSWE in the shallow region above the step patched to linear potential flow in the deep water regions. The corners are located at $x = \pm W/2$, $z = -s$, where $W = 0.5$m and $s = 0.0375$m. The NSWE are solved using the finite volume method with a HLL Riemann solver and MUSCL Hancock scheme. The matching method is the same as that used by Grue (1992) for the Boussinesq model, a source term at the interfaces is used to match the flow. The surface elevation at each edge in the exterior domain is calculated by inputting the flowrate, calculated by the NSWE at the previous timestep, into the matching equation. The surface elevation is then used to force the NSWE by use of a ghost cell at each edge.

The linear heave exciting force on a submerged step is calculated using the theory of Newman et al. (1984), valid for $ks \ll 1$, as shown in Fig. 1a. Three vertical lines are shown at 0.32Hz, 0.421Hz (the first resonance on top of the step, corresponding to the peak in exciting force) and at 0.95Hz corresponding to the frequency used by Grue and later in this work. Figure 1b shows the vertical force on the step calculated using linear potential flow compared to the hybrid NSWE model at these frequencies. At 0.32Hz (Fig. 1b I), away from the resonance, the linear model compares well to the hybrid model except at the troughs. At the resonant frequency (Fig. 1b II) the linear model predicts much larger forces than the hybrid model. It is well known that linear potential flow models tend to over-predict forces at resonances and the same may be occurring here. At 0.95Hz the hybrid model predicts much larger forces. As experimental data for this problem is currently unavailable for the frequencies close to the first resonance, (which are of interest as the CETO device operates in this frequency range) Grue's results at the higher frequency have been used to validate the CFD model and for further comparison to the hybrid model.

3 CFD comparison to experiments

The open source CFD toolbox OpenFoam®, version 2.4.0, has been used in combination with the wave generation and absorption utility waves2Foam (Jacobsen et al., 2012). The two phase flow of water and air is modelled with a VOF scheme for resolving the free surface. The Navier Stokes equations are solved by the finite volume method on a structured multi-block mesh constructed using the blockMesh utility. See Fig. 2 for dimensions of the numerical wave flume. Wave amplitudes in the range of $A_{in}/s = 0.08 - 0.67$ have been considered at a single incident wave frequency. The incident wave frequency is $f = 0.95$Hz (period $T = 1.0526$s), corresponding to wavelength $L = 1.625$m in the deep water region.

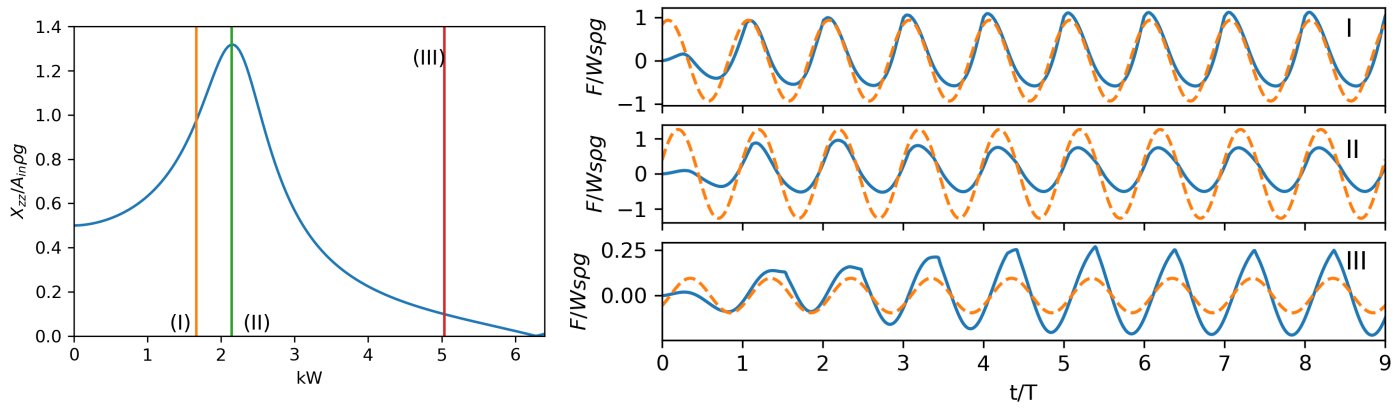

Figure 1: (a) Linear heave exciting force for step with Grue geometry. (b) Vertical force on step, $A_{in}/s = 0.48$, I: $f = 0.32$Hz, II: $f = 0.421$Hz, III: $f = 0.95$Hz. Solid line: hybrid NSWE model, dashed line: linear model.

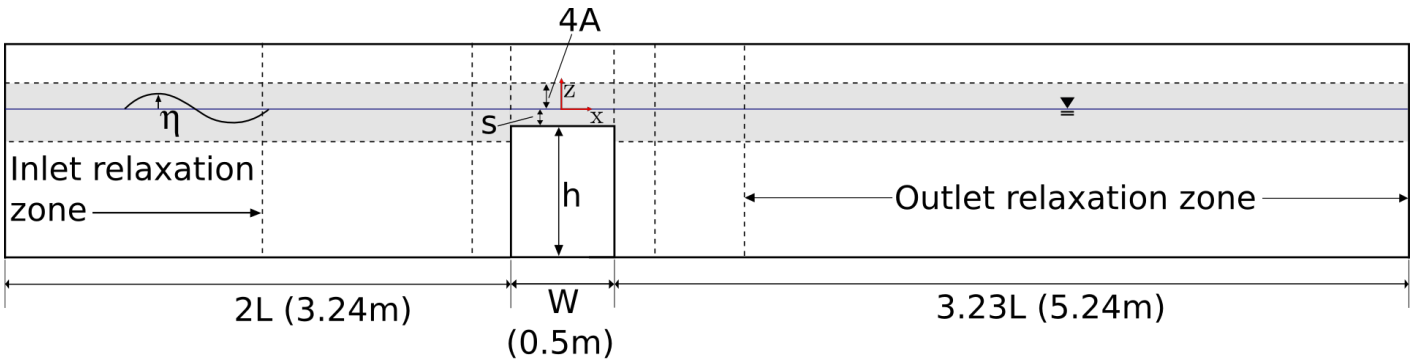

Figure 2: Numerical domain of wave flume (not to scale).

As a means of partial validation, the results of the CFD model are compared to the experimental results of Grue (1992). Fig. 3a shows the first three free harmonic amplitudes in the lee of the step plotted against incident wave amplitude for the present work and Grue's results. The CFD harmonic amplitudes were measured 0.5m down wave of the back (lee) edge of the step, the error bars indicate plus/minus one standard deviation of the harmonic amplitudes measured at the wave gauge by zero crossing analysis, while the markers indicate the mean value. There is good agreement at all amplitudes (over the range considered by Grue) for the first and second harmonic, while the third harmonic measured in the present work is significantly larger than that found in experiments for wave amplitudes less than the spilling limit (The spilling limit was given by Grue at $A_{in}/s = 0.136$). This discrepancy may arise due to the third harmonic not being completely converged with mesh size, although a mesh convergence study suggests the third harmonic to be increasing in amplitude with further mesh refinement. The difference may also result from the sharp corners of the step used in this work, while rounded corners were used by Grue. Fig. 3b shows the variation of the harmonic amplitudes with distance behind the step until the start of the relaxation zone. The transfer of energy from the first harmonic to the higher harmonics can clearly be seen at the back edge of the step, while the drop in the first harmonic amplitude may also be due to reflection at this transition. The harmonics also show some spatial variation of amplitude as they propagate behind the step. However we do not see significant decay in amplitude as might be expected if numerical diffusion was playing a significant role.

4 Surface elevation and force - CFD results

The surface elevation profile as the wave transforms over the step and the total vertical force on the step will be shown for two cases, a relatively small amplitude case where $A_{in}/s = 0.136$ and a larger amplitude, $A_{in}/s = 0.48$, as means of comparison. Figure 4a shows surface elevation snapshots for the smaller amplitude case at two time instants, 1/2 a period apart, averaged over ten wave cycles. The black line shows the mean surface elevation over the ten cycles, while the thinner blue lines indicate the maximum and minimum surface elevation measured at that point over ten cycles. The step is shown in green. Note that the vertical length scale is stretched. The surface elevation measured by the wave gauges is calculated as:

$$\eta(x,t) = \int_{-d(x)}^{\infty} \alpha(x,z,t)\mathrm{d}z - d(x), \tag{1}$$

where $\alpha(x,z,t)$ is the volume fraction of water and air (1 is water, 0 is air) and $d(x)$ is the still water depth as a function of the horizontal coordinate. Thus the surface elevation shown here is a measure of the total height of water above the step at a particular point, not including any air which may become entrained in the flow. Differences in the surface elevation profile between wave

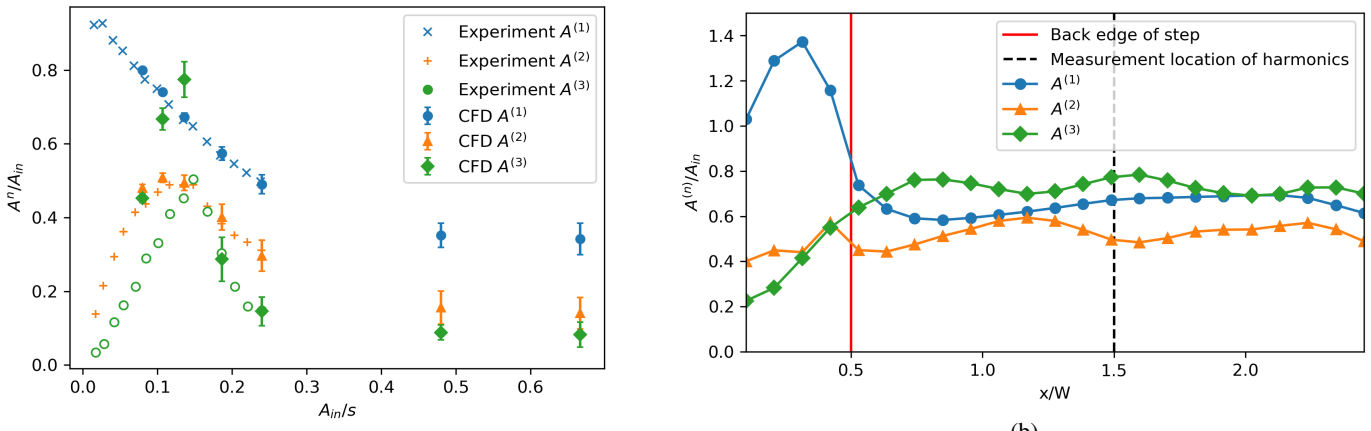

(a) (b)

Figure 3: (a) Harmonic amplitudes measured 0.5m behind the step compared to experimental results from Grue (1992). (b) Harmonic amplitudes with x position behind the step, $A_{in}/s = 0.136$.

periods can be inferred, indicating the wave transformation process is not smooth, irregularity is introduced as the wave "breaks" across the step. The surface elevation to the right of the step shows larger variation between cycles than that to the left due to this process. The steepening of the wave as it transitions onto the step and the generation of higher harmonics as it passes over the step can clearly be seen. Figure 4b shows the surface elevation at two times for the case $A_{in}/s = 0.48$. There is large variation in surface elevation between cycles at the right edge of the step due to wave breaking and air entrainment. The wave also moves below the left edge of the step. For the larger amplitude case it can be seen that the harmonics in the lee of the step are much smaller relative to the wave amplitude and the wave front is steeper on the left side of the step.

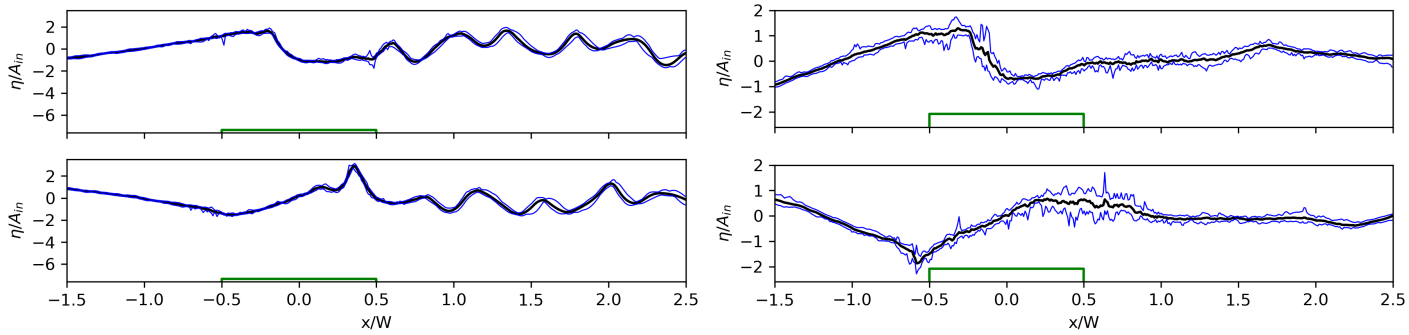

(a) $A_{in}/s = 0.136$ (b) $A_{in}/s = 0.48$

Figure 4: Mean surface elevation at two times, 1/2 a period apart. Note the vertical axis is stretched.

The total vertical force on the step (minus the initial still water force) has been calculated using pressure probes on the step and is compared to the hydrostatic force calculated from the surface elevation measured by the wave gauges, see Fig. 5. The hydrostatic force is calculated as:

$$F(t) = \rho g \int_{x=-W/2}^{x=W/2} \eta(x,t) \mathrm{d}x, \tag{2}$$

where $\eta(x,t)$ is the surface elevation. Note that here a positive value indicates an increase in downward force on the step. In Fig. 5a we see the force for the smaller amplitude case matches the hydrostatic force closely, with some difference at the troughs. It can also be seen that the amplitude of the force changes from cycle to cycle, reflecting the unsteady nature of the flow. Figure 5b shows the force for the case $A_{in}/s = 0.48$, where the hydrostatic force matches the force measured by the probes closely, with the largest discrepancy seen at the peaks. These force results suggest that the flow on top of the step can be modelled as hydrostatic, i.e. vertical accelerations assumed negligible.

5 Hybrid model compared to CFD

Figure 6a shows the surface elevation above the step for the small amplitude case $A_{in}/s = 0.136$ at two time instants, comparing the CFD model (surface elevation averaged over periods) to the NSWE model and results of the Boussinesq model digitised from Grue (1992). In this case the Boussinesq model accurately captures the free surface profile, particularly where the wave steepens at the right side of the step, while the NSWE model shows a steeper wave front travelling faster than predicted by the CFD or Boussinesq

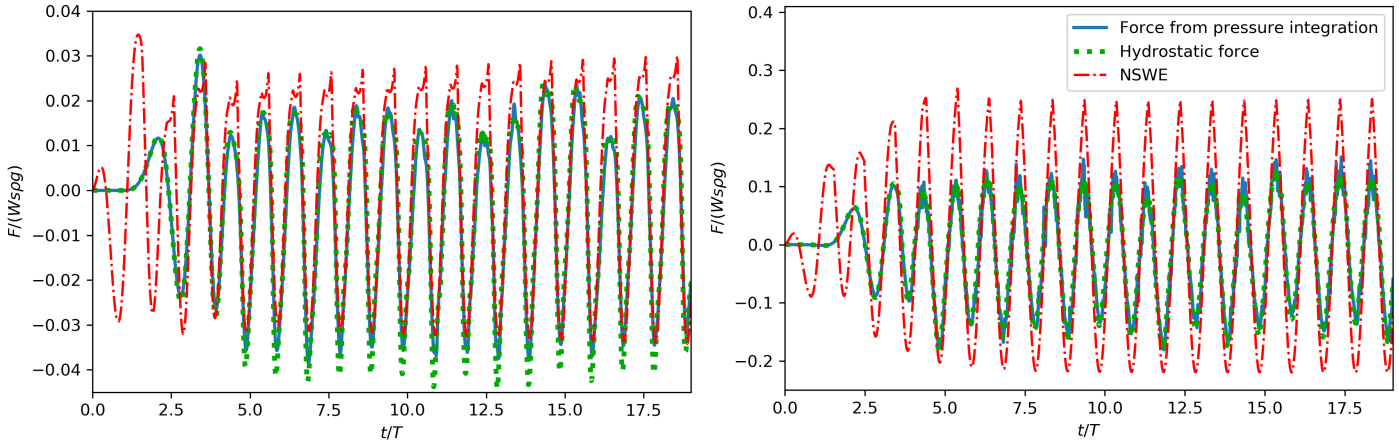

(a) $A_{in}/s = 0.136$ (b) $A_{in}/s = 0.48$

Figure 5: Force on top of the step, from pressure integration, hydrostatic calculations and the hybrid NSWE model.

model. The larger amplitude case is shown in Fig. 6b. In this case the NSWE model predicts large reflection from the downwave end of the step which can be seen propagating right to left as a shock. Comparison of the vertical forces on the step in Fig. 5b indicates that for the case $A_{in}/s = 0.48$ the NSWE model over predicts the flow of water onto and off of the step, resulting in larger amplitude force than given by the CFD. Interestingly the increase in force between Fig. 5a and Fig. 5b appears to be superlinear. Examination of the velocity profiles at the edges indicates that there is a significant vertical component to the velocity at the edges, as well as the horizontal velocity changing direction with depth. The nature of the flow at the edges makes matching at this interface difficult. However the velocity profiles on top of the step further away from the edges show mostly horizontal flow and less variation in magnitude with depth.

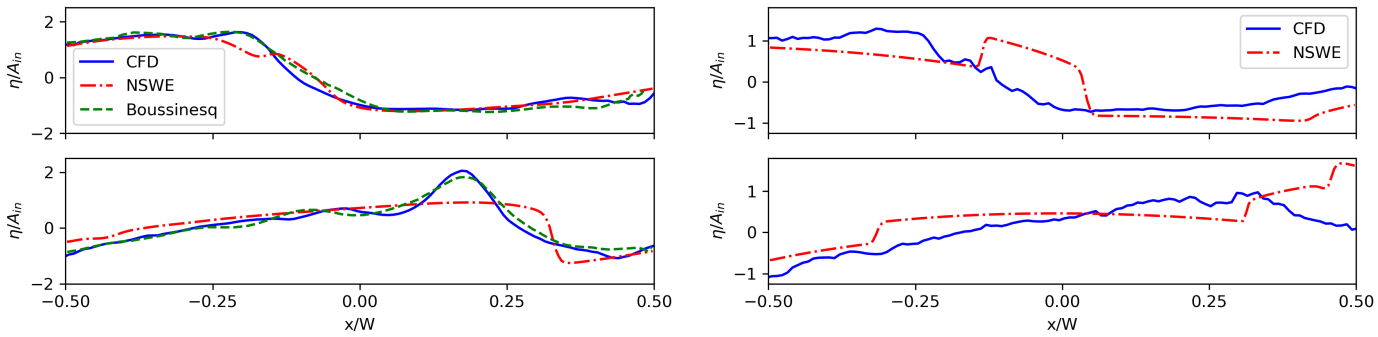

(a) $A_{in}/s = 0.136$ (b) $A_{in}/s = 0.48$

Figure 6: Surface elevation above the step at two time instants 0.35s apart.

6 Conclusion

The transformation of regular waves over a shallowly submerged step has been modelled in CFD with good comparison to experimentally measured harmonics for one incident frequency and several wave amplitudes in the range $A_{in}/s = 0.08 - 0.25$. For larger waves the CFD modelling suggests a rather different regime, with negligible harmonic generation and relatively violent flows on top of the step. The hybrid model performs rather poorly in this amplitude range. However, the CFD does indicate that the flow on top of the step is effectively shallow, suggesting that with appropriate matching at the edges the NSWE could be adequate for this problem. To progress towards a conclusion on the adequacy of such a model, at the workshop further comparisons with CFD at other frequencies will be shown.

References

Grue, J 1992, 'Nonlinear water waves at a submerged obstacle or bottom topography', *J. Fluid. Mech.*, vol. 244, pp. 455–476.

Jacobsen, NG, Fuhrman, DR & Fredsøe, J 2012, 'A wave generation toolbox for the open-source CFD library: OpenFoam®', *Int. J. Num. Meth. in Fluids*, vol. 70, no. 9, pp. 1073–1088.

Newman, J, Sortland, B & Vinje, T 1984, 'Added mass and damping of rectangular bodies close to the free surface', *J. Ship Res.*, vol. 28, no. 4, pp. 219–225.

Skene, DM, Bennetts, LG, Wright, M, Meylan, MH & Maki, KJ 2018, 'Water wave overwash of a step', *J. Fluid. Mech.*, vol. 839, pp. 293–312.